ACCOUNTING FOR DETECTOR CRYSTAL EDGE ROUNDING IN GAMMA-EFFICIENCY CALCULATIONS Theoretical Elaboration and Application in ANGLE Software

by

Nikola MIHALJEVIĆ [1,2]***, Aleksandar DLABAČ*** [2]***, and Slobodan JOVANOVIĆ*** [2, 3*]

[1]Department of Mathematics, Maritime Faculty, University of Montenegro, Kotor, Montenegro
[2] Centre for Nuclear Competence and Knowledge Management, University of Montenegro, Podgorica, Montenegro
[3]Department of Physics, Faculty of Mathematics and Natural Sciences, University of Montenegro, Podgorica, Montenegro

Scientific paper
DOI: 10.2298/NTRP1201001M

In absolute and semi-empirical calculations of full gamma-energy peak efficiencies (ε_p), geometrical/compositional data characterizing the detector should be known in much detail. Among these, detector crystal edge rounding (bulletization), if neglected, may lead to large systematic errors, especially for low gamma-energies and close counting geometries. The errors show quadratic dependence on the extent of bulletization (bulletization radius). Mathematical/analytical solution to the problem – not reported so far – is elaborated in the present work. Relevant mathematical formulae are derived for a number of counting arrangements most frequently encountered in gamma-spectrometry practice (point, disc, cylinder, and Marinelli sources). These are subsequently programmed for numerical calculations and are now part of commercially available ANGLE software. Extensive calculation testing is performed for HPGe (both p- and n-type) and LEPD detectors (several sizes each), with various sources (point, disc, cylinder, Marinelli) and counting geometries (0-20 cm source-to-detector distance). Energy range considered was 10-3000 keV. To elucidate the significance of the issue, an error propagation study was conducted: results with bulletization taken into account are compared to those when bulletization was neglected. Corresponding errors are tabulated in an extensive Excel file. The file comprises about 152 000 error calculation results which are available for download; a few characteristic ones are selected for presenting in the paper. ANGLE proved handy (in programming) and fast (in calculations) when accomplishing this task. The data convincingly illustrate the impact of detector bulletization on gamma-efficiency and thus the need to account for. Even only slight bulletization (1-2 mm bulletization radius) is not negligible in many realistic counting situations. Reader/analyst can (1) compare his/her counting situation with these data so as to get the first impression of the problem and (2) use the mathematical model presented and/or ANGLE software to address the issue.

Key words: detector crystal bulletization, semiconductor detectors, efficiency calculations, error propagation, ANGLE software, gamma-spectrometry

INTRODUCTION

Closed-end coaxial germanium detectors (HPGe, both p- and n-types) are most often manufactured with crystal edges rounded ("bulletized") to some extent, in order to smoothen electric field in the crystal and thus enhance collection of charges produced by X- and gamma-ray interactions (figs. 1 and 2) [1-5]. The same is valid for thick (10-20 mm) semi-planar low-energy photon detectors (LEPD) [1, 8]. Although some manufacturers tend recently to reduce/minimize bulletization of newly produced detectors (because it causes considerable efficiency diminishing at close counting geometries and low energies), the fact is that vast majority of detectors in use do have crystals with rounded edges; bulletization radius is typically in 2-10 mm range (5-50% of the crystal radius) [1-13].

In addition to rounded outer edge of the crystal, inner cavity (crystal hole) is, in general, also rounded for the same reason – improving detector response to X- and gamma-radiation (fig. 1). Both will be further on in the text referred to as detector bulletization.

* Corresponding author; e-mail: bobo_jovanovic@yahoo.co.uk

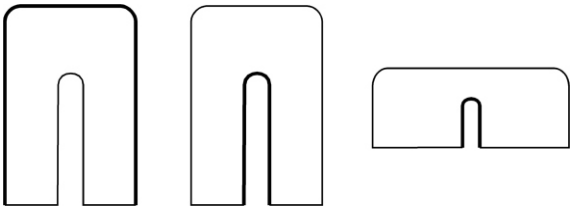

Figure 1. HPGe crystals with rounded edges (bulletized); thick line represents dead Ge layer; p-type HPGe (left), n-type HPGe (middle), and LEPD (right) [1]

Figure 2. Bare HPGe crystal photograph (left), detector radiographies, showing mounted crystal inside (middle and right) [6, 7]; bulletization is clearly seen

In absolute (*e. g.* statistical – Monte Carlo) and semi-empirical (*e. g.* effective solid angle based) calculations of detection efficiency, geometrical and compositional characteristics of the detector are requested as input parameters, one way or the other [15-31]. Due to complex shape and engineering structure of the detector, its mathematical/analytical description (modelling) is always simplified to some extent, *i. e.* systematic error is inevitably introduced into the calculated efficiency. Monte Carlo (MC) simulations offer an advantage in this sense over semi-empirical methods, enabling more versatility and complexity of the description, including bulletization. Even though, dedicated MC codes so far do not offer bulletization option [10]. On the other side, semi-empirical approaches turned out to be generally better suited for the job (efficiency calculations) – offering more practical advantages (better accuracy, less input parameters, much shorter computation times, transparency, user-friendliness and ease-to-use, favorable teaching/training aspects, *etc*.), especially when efficiency transfer (ET) principle is applied [8-10, 26-28, 30].

No exact mathematical/analytical solution was reported so far on the accounting for the effect of crystal bulletization in detector efficiency determination. Estimations invoking the necessity for appropriately dealing with this issue were made on several occasions [7-10]. The same impression we had from the extensive feedback of the users of our ANGLE software for semiconductor detector efficiency calculations and from our own experience [1, 32]. Following this need, we have elaborated an exact mathematical/analytical treatment, which will be presented hereby. The method is incorporated already into ANGLE code [32-34]. For illustration/demonstration purposes, an extensive study was subsequently conceived, exploiting ANGLE ability in easily varying gamma-spectrometry input parameters. Calculations were eventually performed for a large number of possible gamma-spectrometry counting arrangements/situations (about 152 000), elucidating in much detail the practical implications (see further). Results are summarized in such a way that the reader (gamma-spectrometry analyst) can easily estimate the effect/impact of detector bulletization in his/her own conditions – making thus the first step in addressing the problem. Second step – solving the problem – may be applying this approach or just simply using ANGLE software.

THEORETICAL

Full-energy peak detection efficiency (ε_p) can be calculated using the concept of the effective solid angle ($\overline{\Omega}$) [15-17, 35-41]. For a given gamma-source (S) and a semiconductor detector (D) (fig. 3), the effective solid angle is defined as

$$\overline{\Omega} \quad \int_{V_S, S_D} \mathrm{d}\overline{\Omega} \tag{1}$$

where V_S is the source volume, S_D – the detector surface exposed to the source ("visible" by the source), and

$$\mathrm{d}\overline{\Omega} \quad \frac{F_{\mathrm{att}} F_{\mathrm{eff}} \ \mathrm{TP}\ \vec{n}_u}{|\mathrm{TP}|^3} \mathrm{d}\sigma \tag{2}$$

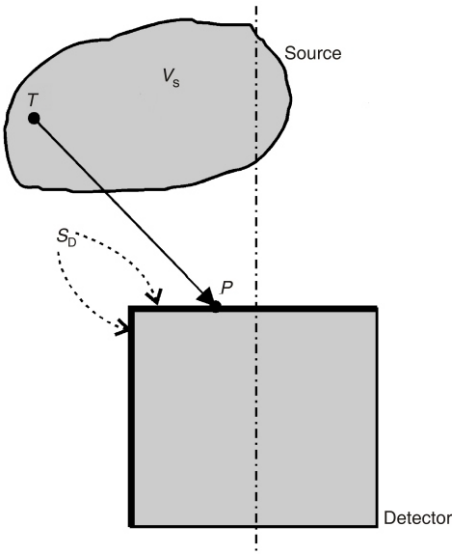

Figure 3. To the definition of the effective solid angle ($\overline{\Omega}$), eq. (1)

Here T is the point varying over V_S, P – the point varying over S_D, and $\vec{n}_u$ the external unit vector normal to infinitesimal area $\mathrm{d}\sigma$ at S_D. Equation (1) is thus a five fold integral. Factor F_{att} accounts for gamma attenuation of the photon following the direction TP out of the

detector active zone, while F_{eff} describes the probability of an energy degradable photon interaction with the active detector body (*i. e.* coherent scattering excluded), initiating the detector response. The two factors include therefore geometrical and composition-related parameters of the materials traversed by the photon.

Full-energy peak detection efficiency (ε_{p}) is subsequently found as

$$\varepsilon_{\text{p}} \quad \frac{P}{T}\overline{\Omega} \tag{3}$$

where P/T is the "virtual" peak-to-total ratio ("virtual" meaning it is valid for a bare isolated detector crystal in a vacuum) [15]. Fairly assuming that P/T is an intrinsic characteristic of the detector crystal (depending on gamma-energy only) [36, 41, 42], implies that ε_{p} is proportional to $\overline{\Omega}$. This proportionality enables simple conversion from the chosen (say known – accurate and reliably determined) reference geometry (index ref) – to that of the actual sample (unknown efficiency)

$$\varepsilon_{\text{p}} \quad \varepsilon_{\text{p,ref}} \frac{\overline{\Omega}}{\overline{\Omega}_{\text{ref}}} \tag{4}$$

Note that with such conversion (efficiency transfer – ET), assumption of P/T constancy is practically extended (for efficiency determination) beyond its literal meaning – thanks to partial error compensation in $\overline{\Omega}/\overline{\Omega}_{\text{ref}}$ ratio. The more the actual sample and counting geometry resemble the reference ones, the more this stands.

For the purpose of the present work, ε_{p} to $\overline{\Omega}$ proportionality helps to derive conclusions about ε_{p} variations/behavior by analyzing those of $\overline{\Omega}$.

Detector crystal edge rounding (bulletization) is defined by its radius ρ ($0 < \rho < R_0$, with R_0 the detector radius, $R_0 < H$, fig. 4). When applying eqs. (1) and (2) to a point source T and bulletized closed-end coaxial HPGe detector, we obtain

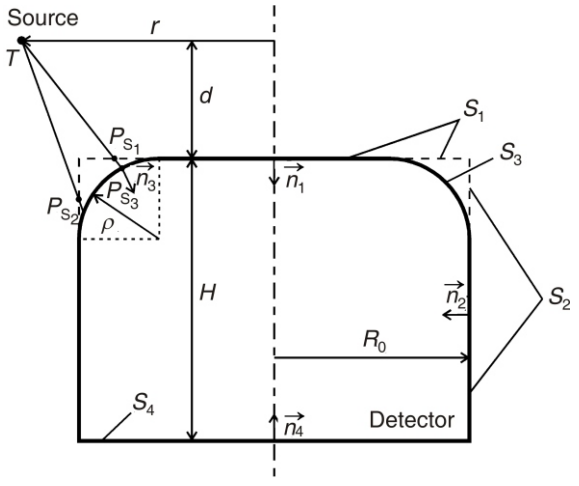

Figure 4. To the calculation of $\overline{\Omega}$ for point source and bulletized detector, eq. (3)

$$\overline{\Omega} \quad 2\int_0^{\pi}\mathrm{d}\theta\int_{\theta_0}^{R_0} F_{\text{att}}F_{\text{eff}}F_1(T,P_{S_1})R\,\mathrm{d}R \\ +2R_0\int_0^{0}\mathrm{d}\theta\int_{-H}^{0} F_{\text{att}}F_{\text{eff}}F_2(T,P_{S_2})\,\mathrm{d}h \tag{5}$$

with $T(r, 0, d)$, $P_{S_1} = (R\cos\theta \;\; R\sin\theta \quad , P_{S_2} = (R_0\cos\theta, R_0\sin\theta \quad h)$ and, $\theta_0 = \arctan[(r^2 \quad R_0^2)^{1/2}/R_0]$ while functions F_1 and F_2 are given as

$$\frac{\mathrm{TP}_{S_1}\;\vec{\mathrm{n}}_1}{\left|\mathrm{TP}_{S_1}\right|^3}, \quad R \quad R_0 \quad \rho$$

$$F_1(T,P_{S_1}) \quad \frac{\mathrm{TP}_{S_3}\;\vec{\mathrm{n}}_3}{\left|\mathrm{TP}_{S_3}\right|^3}, \quad R \quad R_0 \quad \rho \quad TP_{S_1} \quad S_3$$

$$0, \qquad R \quad R_0 \quad \rho \quad TP_{S_1} \quad S_3 \tag{6}$$

with $\vec{\mathrm{n}}_1 \quad (0,0, \quad 1)$, $P_{S_3} \quad TP_{S_1} \quad S_3$ and $\vec{\mathrm{n}}_3 \quad \vec{\mathrm{n}}_3(P_{S_3})$

$$\frac{\mathrm{TP}_{S_2}\;\vec{\mathrm{n}}_2}{\left|\mathrm{TP}_{S_2}\right|^3}, \quad h \quad \rho$$

$$F_2(T,P_{S_2}) \quad \frac{\mathrm{TP}_{S_3}\;\vec{\mathrm{n}}_3}{\left|\mathrm{TP}_{S_3}\right|^3}, \quad h \quad \rho \quad TP_{S_2} \quad S_3$$

$$0, \qquad h \quad \rho \quad TP_{S_2} \quad S_3 \tag{7}$$

with $\vec{\mathrm{n}}_2 \quad (\cos\theta, \quad \sin\theta, 0)$, $P_{S_3} \quad TP_{S_2} \quad S_3$ and $\vec{\mathrm{n}}_3 \quad \vec{\mathrm{n}}_3(P_{S_3})$

Thus, co-ordinates of point P_{S_3} are obtained as the cross-section of straight line TP (where $P \quad P_{S_1}$ or $P \quad P_{S_2}$), defined by the equation

$$TP\text{:} \quad \frac{x \quad x_{\text{T}}}{x_{\text{P}} \quad x_{\text{T}}} \quad \frac{y \quad y_{\text{T}}}{y_{\text{P}} \quad y_{\text{T}}} \quad \frac{z \quad z_{\text{T}}}{z_{\text{P}} \quad z_{\text{T}}} \tag{8}$$

and surface S_3 (detector curvature), which is geometrically represented as a part of the torus defined by the equation

$$S_3\text{:} \quad 4(R_0 \quad \rho)^2(x^2 \quad y^2) \\ [x^2 \quad y^2 \quad (z \quad \rho)^2 \quad (R_0 \quad \rho)^2 \quad \rho^2]^2 \tag{9}$$

Substituting eq. (8) into eq. (9), yields a fourth order algebraic equation. Solution to this equation is analytically obtained using Ferrari's algorithm [43].

In the above, co-ordinates of normal vector $\vec{n}_3 = (n_x, n_y, n_z)$ are:

$$n_x \quad \frac{x_c \quad x_3}{\rho}, n_y \quad \frac{y_c \quad y_3}{\rho}, n_z \quad \frac{\rho \quad z_3}{\rho}$$

with x_3, y_3 and z_3 denoting co-ordinates of point P_{s_3}, and

$$x_c \quad \frac{x_3 s}{x_3^2 \quad y_3^2}, y_c \quad \frac{s \quad x_3 x_c}{y_3},$$

$$s \quad \frac{(R_0 \quad \rho)^2 \quad x_3^2 \quad y_3^2 \quad z_3^2 \quad 2\rho z_3}{2}$$

Note that if $|y_3| \quad \varepsilon (\varepsilon \quad 0$ is a small number), then

$$y_c \quad \frac{y_3 s}{x_3^2 \quad y_3^2}, x_c \quad \frac{s \quad y_3 y_c}{x_3}$$

thus avoiding division by a close-to-zero number.

Applying the above mathematical reasoning to some characteristic sources and counting geometries typically encountered in gamma-spectrometry practice with semiconductor detectors, the following can be obtained (for symbols used to denote intervals of integration, see the corresponding figures).

Disc source (coaxially positioned with detector, fig. 5)

$$\overline{\Omega} \quad \underset{(Q_1 \quad Q_2),\, S_1}{\mathrm{d}\overline{\Omega}} \quad \underset{Q_2,\, S_2}{\mathrm{d}\overline{\Omega}} \tag{10}$$

or

$$\overline{\Omega} \quad \frac{4}{r_0^2} \int_0^{r_0} r\mathrm{d}r \int_0^{\pi} \mathrm{d}\theta \int_0^{R_0} F_{\mathrm{att}} F_{\mathrm{eff}} F_1(T, P_{s_1}) R\mathrm{d}R$$
$$\frac{4R_0}{r_0^2} \int_{R_0}^{r_0} r\mathrm{d}r \int_0^{\theta_0} \mathrm{d}\theta \int_H^0 F_{\mathrm{att}} F_{\mathrm{eff}} F_2(T, P_{s_2}) \mathrm{d}h \tag{11}$$

Cylindrical source (coaxially positioned with detector, fig. 6)

$$\overline{\Omega} \quad \underset{(V_1 \quad V_2),S_1}{\mathrm{d}\overline{\Omega}} \quad \underset{V_2,S_2}{\mathrm{d}\overline{\Omega}} \tag{12}$$

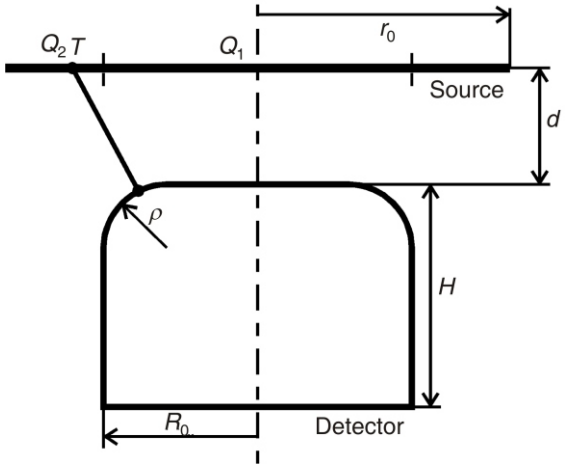

Figure 5. To the calculation of $\overline{\Omega}$ for disc source and bulletized detector, eq. (10)

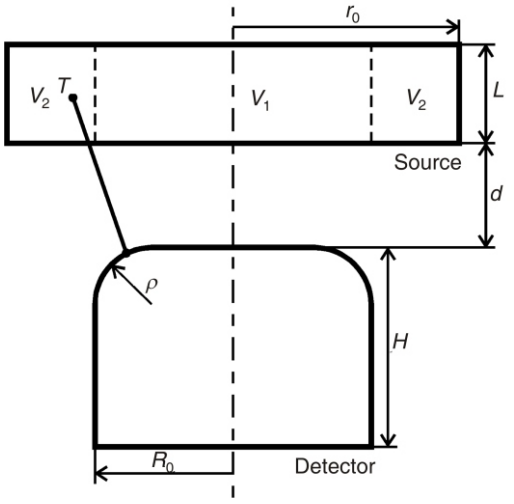

Figure 6. To the calculation of $\overline{\Omega}$ for cylindrical source and bulletized detector, eq. (12)

or

$$\overline{\Omega} \quad \frac{4}{r_0^2 L} \int_0^L \mathrm{d}l \int_0^{r_0} r\mathrm{d}r \int_0^{\pi} \mathrm{d}\theta \int_0^{R_0} F_{\mathrm{att}} F_{\mathrm{eff}} F_1(T, P_{S_1}) R\mathrm{d}R$$
$$\frac{4R_0}{r_0^2 L} \int_0^L \mathrm{d}l \int_{R_0}^{r_0} r\mathrm{d}r \int_0^{\theta_0} \mathrm{d}\theta \int_H^0 F_{\mathrm{att}} F_{\mathrm{eff}} F_2(T, P_{S_2}) \mathrm{d}h \tag{13}$$

with $T(r, 0, d + l)$.

Equations (10)-(13) are valid for sources with radii larger than that of the detector ($r_0 > R_0$); for smaller sources ($r_0 < R_0$) second term integrals are omitted.

Marinelli geometry is described by

$$\overline{\Omega} \quad \underset{(V_1 \quad V_2),S_1}{\mathrm{d}\overline{\Omega}} \quad \underset{V_2,S_2}{\mathrm{d}\overline{\Omega}} \quad \underset{V_3,S_1}{\mathrm{d}\overline{\Omega}} \quad \underset{(V_3 \quad V_4 \quad V_5),S_2}{\mathrm{d}\overline{\Omega}} \quad \underset{V_5,S_4}{\mathrm{d}\overline{\Omega}} \tag{14}$$

which gives

$$\overline{\Omega} \quad \frac{4}{W} \int_0^L \mathrm{d}l \int_0^{r_0} r\mathrm{d}r \int_0^{\pi} \mathrm{d}\theta \int_0^{R_0} F_{\mathrm{att}} F_{\mathrm{eff}} F_1(T, P_{S_1}) R\mathrm{d}R$$
$$+ \frac{4R_0}{W} \int_0^L \mathrm{d}l \int_{R_0}^{r_0} r\mathrm{d}r \int_0^{\theta_0} \mathrm{d}\theta \int_H^0 F_{\mathrm{att}} F_{\mathrm{eff}} F_2(T, P_{S_2}) \mathrm{d}h$$
$$\frac{4}{W} \int_0^d \mathrm{d}l \int_{r_\varphi}^{r_0} r\mathrm{d}r \int_0^{\pi} \mathrm{d}\theta \int_0^{R_0} F_{\mathrm{att}} F_{\mathrm{eff}} F_1(T_{\mathrm{m}}, P_{S_1}) R\mathrm{d}R$$
$$\frac{4R_0}{W} \int_{d \quad L\varphi}^d \mathrm{d}l \int_{r_\varphi}^{r_0} r\mathrm{d}r \int_0^{\theta_0} \mathrm{d}\theta \int_H^0 F_{\mathrm{att}} F_{\mathrm{eff}} F_2(T_{\mathrm{m}}, P_{S_2}) \mathrm{d}h$$
$$\frac{4}{W} \int_{d \quad L\varphi}^H \mathrm{d}l \int_{r_\varphi}^{r_0} r\mathrm{d}r \int_0^{\pi} \mathrm{d}\theta \int_0^{R_0} F_{\mathrm{att}} F_{\mathrm{eff}} F_4(T_{\mathrm{m}}, P_{S_4}) R\mathrm{d}R \tag{15}$$

where

$$W \quad r_0^2 L \quad (r_0^2 \quad r_\varphi^2) L_\varphi, T(r, 0, d \quad l),$$
$$T_{\mathrm{m}}(r, 0, l), P_{s_4}(R\cos\theta, R\sin\theta, \quad H)$$

and function F_4 is described by

$$F_4(T, P_{S_4}) \quad \frac{\mathrm{TP}_{S_4} \vec{n}_4}{|TP_{S_4}|^3} \text{ with } \vec{n}_4 \quad (0,0,1) \tag{16}$$

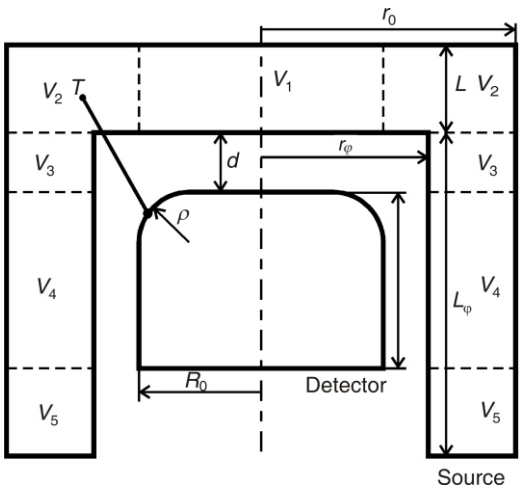

Figure 7. To the calculation of $\overline{\Omega}$ for Marinelli source and bulletized detector, eq. (14)

Note that in further elaboration of the mathematical analysis, rounding of the crystal core (hole) was also taken into account – appropriate relations are contained within F_{eff} factor. It is assumed that core bulletization radius is equal to hole radius, as is normally the case in practice (fig. 1). Being one of many details describing the detector, and having in mind extremely extensive final formulae, this is not felt necessary to be presented more minutely hereby.

For thick LEPD (fig. 1), which have essentially the same configuration as closed-end coaxial n-type HPGe detectors, same equations as the above derived ones are valid. If $R_0 > H$, as usual with LEPD, then $0 < \rho < H$ (thus not $0 < \rho < R_0$).

Since ε_p is directly proportional to $\overline{\Omega}$, eq. (3), further conclusions about $\overline{\Omega}$ are applicable to ε_p – as long as the proportionality holds, of course [36, 41, 42]. Note that when the efficiency transfer (ET) principle is used for efficiency calculations, the impact of the uncertainties in detector data (error propagation) tends to reduce due to partial cancelling, eq. (4), [11, 12, 27, 28]; as a matter of fact, this applies also to bulletization. The more actual sample (shape, size, matrix, beaker) and counting geometry (source-to-detector position/distance) are close to reference ones, the more such error reduction is prominent. In this sense – as previously suggested – ET-principle beneficially expands $\overline{\Omega}$ applicability to ε_p calculations in regions where the two incline to slipping out of the proportionality range (*e. g.* at low gamma-energies for HPGe detectors, high gamma-energies for LEPD, for bulky sources at close geometries, *etc.*).

Finally, one should bear in mind that – when regarding the same detector with and without bulletization – P/T is, strictly speaking, not concerning the same detector anymore. In exact terms, the ε_p *vs.* $\overline{\Omega}$ proportionality assumption should be adjusted in this respect. For the purpose of the present work this nuance will be neglected, since the conclusions to be derived on bulletization error propagation, see further, eq. (17), are anyhow of indicative/illustrative nature only. The same observation holds, after all, for analogue error propagation studies of other detector parameters (*e. g.* dimensions of the crystal itself, dead layers, vacuum, end-cap, low-Z window, housing, *etc.*) [15].

Needless to say, the above does not affect the exactness of the mathematical approach, eqs. (5)-(16) – when calculating detection efficiencies using ET principle, eq. (4), it always goes about the same one detector. In general, as far as realistic situations in gamma-spectrometry are concerned, we are on the safe side – no major/unacceptable strays due to P/T-constancy assumption are expected.

APPLICATION IN ANGLE COMPUTER CODE

The above formulae were first incorporated by 2009 into version 2.1 of ANGLE, our efficiency calculation software (commercially available) and, later on – with enhanced precision and calculation speed – into current version 3.0 [32-34]. A typical ANGLE screen (including bulletization data input) is given in fig. 8.

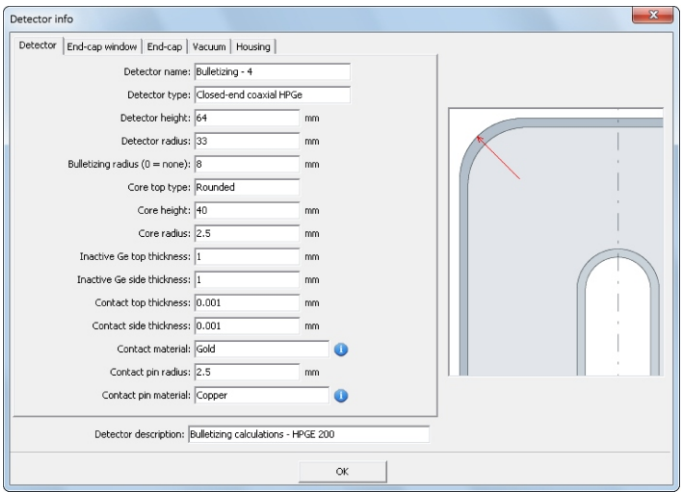

Figure 8. ANGLE screen illustrating data input, including crystal bulletization

The software offers comfortable, transparent, comprehensive and fast data manipulation, both for input and output. Besides its primary function (efficiency calculations), it enables *inter alia* easy and illustrative error propagation investigations – that is to say observing the impact of input parameter variations on the final gamma-spectrometry result. For the purpose of the present work it served to bulletization study, as follows.

PRACTICAL IMPLICATIONS AND DISCUSSION

The effect of detector crystal bulletization on the effective solid angle ($\overline{\Omega}$) – and hence on the ε_p-calculation result, eqs. (3) and (4) – is studied by entering into calculations various input parameters, namely:

- detector types and sizes (tab. 1)
  - HPGe p-type (volume = 100, 200, and 500 cm^3),
  - HPGe n-type (volume = 100, 200, and 500 cm^3), and
  - thick LEPD (thickness = 10 and 20 mm),
- bulletization radius (ρ/R_0 = 0-100%, in 5% increments),
- source types and volumes (tab. 2)
  - point,
  - disc (radius = 1, 2, 5, 10, and 20 cm),
  - cylinder (volume = 10, 100, and 1000 ml), and
  - Marinelli (200, 500, 1000, 2000, and 5000 ml),
- source matrices (water, epoxy resin $C_{21}H_{25}ClO_5$ 1.4 g/cm^3, carbonate rock $CaCO_3$ 2.71 g/cm^3),
- counting geometries (source to detector end-cap distance = 0, 10, and 20 cm), and
- gamma-energies (16 energies in 10-3000 keV range).

Some of these are characteristically met in gamma-spectrometry practice, while the others are rather theoretical. The latter case concerns *e. g.* extremely bulletized crystals ($\rho/R_0 > 50\%$) or situations of very low efficiencies (for instance counting with p-type HPGe detectors below 50 keV or with LEPD above 500 keV).

Results are compared to $\overline{\Omega}$-values with no bulletization taken into account ($\rho = 0$). Relative discrepancies (in %) are then calculated as

$$\delta[\%] \quad \left| \frac{\overline{\Omega}(0)}{\overline{\Omega}(\rho)} \quad 1 \right| 100 \qquad (17)$$

Since $\overline{\Omega}(0)/\overline{\Omega}(\rho$ ε_{p} $\varepsilon_{\mathrm{p}}\,\rho$ δ-values are the errors made in the efficiency calculations by not taking bulletization into account.

With all combinations of the above input parameters (detector, source, geometry, gamma-energy, bulletization radius, *etc*.), a total of 152 640 $\overline{\Omega}$-calculations were performed using ANGLE 3 software. Relevant δ-values, eq. (17), are systematized per detector-source-matrix-distance in 480 tables in an Excel file, each table (except for 10 mm LEPD) consist-

Table 1. Characteristics of the detectors used in the study

Detector Parameter [mm]	Thick LEPD 10 mm	Thick LEPD 20 mm	HPGe p-type 100 cm^3	HPGe p-type 200 cm^3	HPGe p-type 500 cm^3	HPGe n-type 100 cm^3	HPGe n-type 200 cm^3	HPGe n-type 500 cm^3
Crystal radius	18	18	26	33	44	25	32	43
Crystal height	10	20	52	64	87	52	63	87
Dead layer	0.001	0.001	1	1	1	0.001	0.001	0.001
Core height	5	5	30	40	60	30	40	60
Core radius	1.5	1.5	2.5	2.5	2.5	2.5	2.5	2.5
Contact thickness	1	1	0.001	0.001	0.001	1	1	1
Crystal to end cap distance	5	5	5	5	5	5	5	5
End cap thickness (Al)	1	1	1	1	1	1	1	1
Window thickness (Be)	0.5	0.5	0.5	0.5	0.5	0.8	0.5	0.5

Table 2. Characteristics of voluminous sources used in the study

Source Parameter [mm]	Cylinder 10 ml	Cylinder 100 ml	Cylinder 1 l	Marinelli 200 ml	Marinelli 500 ml	Marinelli 1 l	Marinelli 2 l	Marinelli 5 l
Height	17	38	83	76	84	93	107	135
Radius	14	29	62	56	64	73	87	115
Cavity height	–	–	–	70	70	70	70	70
Cavity radius	–	–	–	49	49	49	49	49
Contact wall thickness (plastic)	1	1	1	1	1	1	1	1

ing of 336 calculation results (16 energies for each of 21 ρ/R_0 values). The file is too extensive to be presented integrally as a part of this article, but can be downloaded from ANGLE Web site [44]. For illustration, some of its constituent tables are given in tab. 3 in reduced forms (ρ/R_0 50%; E_γ 50 keV for p-type HPGe; E_γ 500 keV for LEPD). In fig. 9 examples of graphical representation of the tabulated δ-values are shown – for better perception and easier concluding.

It should be noted that – despite huge number of input files (nearly 10 000 required to be prepared for ANGLE calculations) – this study was relatively simple and easy to program (one day work), benefiting from the software built-in options for gamma-spectrometry studies. Total calculation time was less than 10 hours on a HP EliteBook 8540p laptop computer (by utilizing all four processor cores at the same time), *i. e.* only 0.23 seconds on average per $\overline{\Omega}$-value and gamma-energy of interest. Calculation time is so short thanks to the calculation optimization built in ANGLE 3, whereby an order of magnitude (or even two) saving in computation time is achieved. Note that the same study (*i. e.* the same amount of calculation) using MC codes, especially with comparable calculation precision ($<10^{-5}$), would be practically impossible – taking months, even years.

Clearly and convincingly results in tab. 3 confirm the necessity for taking crystal bulletization into account in detector efficiency calculations. Let us only pay attention to a few typical situations which illustrate this:

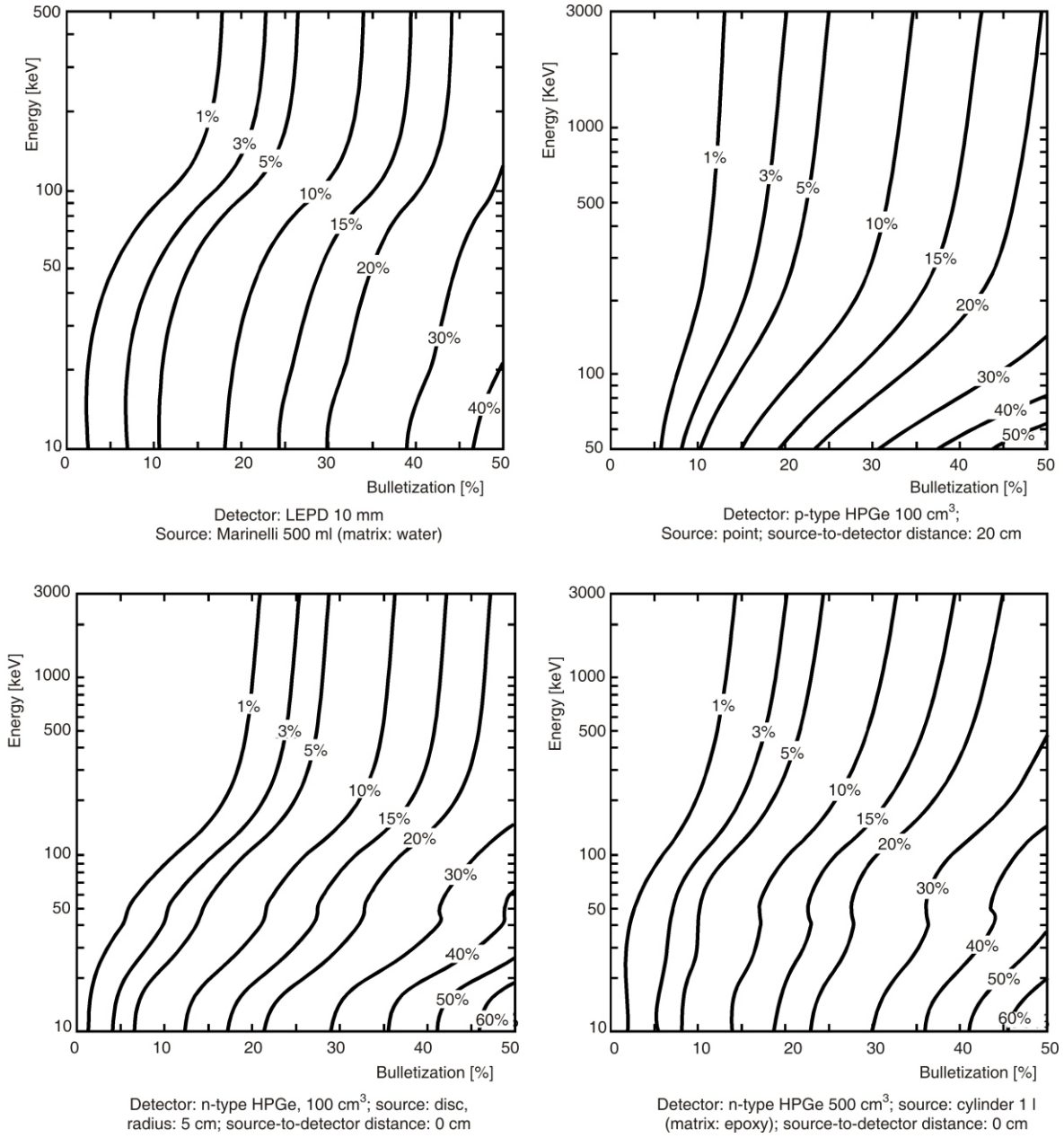

Figure 9. Isometric error representation, illustrating four cases from tab. 3

Table 3. Examples of errors (δ, in %) made in $\overline{\Omega}$ calculations (and consequently in ε_p) by not taking detector crystal bulletization into account, eq. (17), for various detectors, sources, and counting geometries; $\beta = \rho/R_0$ (in %) is a measure of the bulletization; E_γ is in keV; the data presented are excerpted from extensive Excel file containing 480 tables with 152 640 calculated δ-values, downloadable from ref. [44]

Detector: LEPD 10 mm

Source: point; distance : 0 cm

$E_\gamma \mid \beta$	5	10	15	20	25	30	35	40	45	50
10	1.8	3.7	5.9	8.4	11.4	14.8	18.4	22.2	27.3	33.9
15	1.8	3.8	6.0	8.5	11.5	14.9	18.6	22.5	27.6	34.1
20	1.9	3.9	6.2	8.8	11.8	15.4	19.1	23.1	28.3	35.1
30	1.7	3.7	6.1	8.8	11.9	15.5	19.1	23.2	28.5	35.4
50	1.1	3.0	5.2	7.8	10.8	14.5	18.2	22.1	27.4	34.2
70	0.6	2.1	3.9	6.2	9.0	12.3	16.0	19.8	24.8	31.4
100	0.3	1.3	2.6	4.3	6.5	9.3	12.5	15.9	20.3	26.0
150	0.2	0.9	1.8	3.2	5.0	7.2	9.9	12.9	16.7	21.8
200	0.2	0.8	1.6	2.9	4.5	6.6	9.1	12.0	15.6	20.4
300	0.2	0.7	1.5	2.7	4.2	6.2	8.6	11.4	14.9	19.5
500	0.2	0.7	1.4	2.5	4.0	5.9	8.3	11.0	14.5	19.0

Source: Marinelli 500 ml, matrix: water

$E_\gamma \mid \beta$	5	10	15	20	25	30	35	40	45	50
10	2.0	4.6	7.7	11.3	15.5	20.2	25.5	31.4	37.9	45.2
15	2.1	4.6	7.5	10.8	14.6	18.8	23.4	28.6	34.3	40.6
20	1.8	4.0	6.5	9.4	12.7	16.3	20.3	24.8	29.7	35.0
30	1.4	3.4	5.7	8.3	11.2	14.5	18.2	22.2	26.6	31.5
50	0.7	2.5	4.6	7.1	10.0	13.2	16.7	20.6	24.9	29.7
70	0.1	1.4	3.3	5.7	8.4	11.5	15.0	18.9	23.3	28.2
100	0.3	0.4	1.8	3.7	6.2	9.1	12.6	16.6	21.2	26.5
150	0.6	0.3	0.8	2.4	4.7	7.6	11.1	15.3	20.2	26.0
200	0.7	0.5	0.5	2.1	4.3	7.2	10.7	15.0	20.1	26.1
300	0.7	0.6	0.3	1.9	4.1	7.0	10.5	14.8	20.0	26.1
500	0.8	0.7	0.2	1.7	3.9	6.8	10.4	14.7	19.9	26.1

Detector: LEPD 20 mm

Source: disc 20 cm radius; distance: 10 cm

$E_\gamma \mid \beta$	5	10	15	20	25	30	35	40	45	50
10	1.8	3.8	5.9	8.3	10.8	13.4	16.1	19.1	22.3	25.6
15	1.8	3.8	5.8	8.1	10.5	13.0	15.7	18.6	21.6	24.9
20	1.4	3.0	4.7	6.6	8.5	10.6	12.8	15.2	17.6	20.2
30	0.8	2.0	3.2	4.5	5.9	7.4	9.0	10.7	12.5	14.3
50	0.1	0.9	1.9	3.0	4.2	5.5	6.8	8.2	9.7	11.2
70	0.4	0.0	0.8	1.7	2.8	3.9	5.2	6.5	7.9	9.4
100	0.8	0.9	0.7	0.1	0.6	1.5	2.6	3.8	5.0	6.4
150	1.1	1.6	1.8	1.6	1.2	0.6	0.2	1.2	2.4	3.7
200	1.2	1.8	2.2	2.1	1.9	1.3	0.6	0.4	1.5	2.9
300	1.3	2.0	2.4	2.5	2.3	1.8	1.1	0.1	1.0	2.5
500	1.3	2.1	2.6	2.7	2.5	2.1	1.4	0.5	0.7	2.2

Source: cylinder 10 ml (matrix: epoxy); distance: 10 cm

$E_\gamma \mid \beta$	5	10	15	20	25	30	35	40	45	50
10	3.6	7.3	11.1	15.3	19.5	24.0	28.6	33.5	38.5	43.8
15	3.7	7.5	11.4	15.6	19.9	24.4	29.1	34.1	39.2	44.6
20	3.6	7.3	11.1	15.2	19.4	23.9	28.5	33.3	38.4	43.6
30	3.4	7.0	10.8	14.8	19.0	23.4	27.9	32.6	37.6	42.7
50	2.7	6.3	9.9	13.9	18.0	22.3	26.8	31.5	36.3	41.4
70	2.0	5.2	8.7	12.5	16.5	20.7	25.1	29.7	34.5	39.4
100	1.2	3.7	6.7	10.2	13.9	17.8	22.0	26.3	30.9	35.7
150	0.8	2.6	5.0	8.0	11.3	15.0	18.9	23.2	27.7	32.4
200	0.6	2.2	4.4	7.2	10.4	14.0	17.9	22.1	26.6	31.5
300	0.5	2.0	4.1	6.8	9.9	13.4	17.2	21.5	26.0	30.9
500	0.5	1.8	3.9	6.5	9.5	13.0	16.9	21.1	25.7	30.6

Detector: p-type HPGe 100 cm^3

Source: point; distance: 20 cm

$E_\gamma \mid \beta$	5	10	15	20	25	30	35	40	45	50
50	0.4	4.7	10.1	15.9	22.2	28.9	36.2	43.9	52.3	61.3
70	0.2	3.4	7.5	12.1	16.9	22.1	27.6	33.3	39.4	45.8
100	0.1	2.2	5.3	9.1	13.0	17.2	21.7	26.4	31.2	36.3
150	0.0	1.3	3.6	6.5	9.7	13.3	17.1	21.1	25.3	29.8
200	0.0	1.0	2.9	5.4	8.3	11.5	15.0	18.8	22.7	26.9
300	0.0	0.8	2.3	4.5	7.1	10.1	13.4	16.9	20.6	24.6
500	0.0	0.6	2.0	3.9	6.3	9.1	12.3	15.6	19.2	23.1
700	0.0	0.6	1.9	3.7	6.0	8.7	11.7	15.0	18.6	22.4
1000	0.0	0.5	1.7	3.5	5.7	8.3	11.2	14.5	18.0	21.8
1500	0.0	0.5	1.6	3.2	5.3	7.9	10.8	14.0	17.4	21.1
2000	0.0	0.5	1.5	3.1	5.2	7.6	10.5	13.7	17.1	20.8
3000	0.0	0.4	1.5	3.0	5.0	7.4	10.3	13.4	16.8	20.5

Source: cylinder 100 ml (matrix: water); distance: 0 cm

$E_\gamma \mid \beta$	5	10	15	20	25	30	35	40	45	50
50	0.2	3.7	8.5	13.8	19.7	26.1	33.0	40.5	48.7	57.6
70	0.1	2.5	6.5	11.2	16.6	22.5	29.0	36.2	43.9	52.4
100	0.0	1.5	4.3	8.0	12.4	17.5	23.3	29.7	36.7	44.5
150	0.0	0.8	2.7	5.4	8.7	12.7	17.3	22.6	28.5	35.2
200	0.0	0.7	2.2	4.4	7.3	10.8	14.9	19.6	24.9	30.9
300	0.0	0.5	1.8	3.8	6.3	9.4	13.1	17.4	22.2	27.8
500	0.0	0.5	1.6	3.4	5.7	8.6	12.0	16.0	20.5	25.7
700	0.0	0.4	1.5	3.2	5.4	8.2	11.5	15.3	19.7	24.8
1000	0.0	0.4	1.4	3.0	5.2	7.8	11.0	14.7	19.0	23.9
1500	0.0	0.4	1.4	2.9	4.9	7.5	10.5	14.1	18.3	23.0
2000	0.0	0.3	1.3	2.8	4.8	7.3	10.3	13.8	17.9	22.6
3000	0.0	0.3	1.3	2.7	4.7	7.1	10.1	13.5	17.5	22.1

Detector: p-type HPGe 200 cm^3

Source: disc 20 cm radius; distance: 0 cm

$E_\gamma \mid \beta$	5	10	15	20	25	30	35	40	45	50
50	0.5	0.2	0.4	1.7	3.2	4.8	6.7	9.0	11.0	13.4
70	0.4	0.4	0.1	1.2	2.7	4.3	6.2	8.5	10.7	13.2
100	0.4	0.5	0.0	1.0	2.5	4.1	6.1	8.4	10.7	13.4
150	0.3	0.6	0.2	0.7	2.0	3.6	5.6	7.9	10.3	13.0
200	0.3	0.7	0.4	0.5	1.7	3.3	5.2	7.5	9.9	12.7
300	0.3	0.7	0.5	0.3	1.5	3.1	5.0	7.2	9.7	12.5
500	0.3	0.8	0.5	0.2	1.4	2.9	4.8	7.1	9.5	12.3
700	0.4	0.8	0.6	0.2	1.4	2.9	4.7	7.0	9.5	12.3
1000	0.4	0.8	0.6	0.1	1.3	2.8	4.7	7.0	9.4	12.3
1500	0.4	0.8	0.6	0.1	1.3	2.8	4.7	7.0	9.4	12.3
2000	0.4	0.8	0.6	0.1	1.2	2.7	4.6	7.0	9.4	12.4
3000	0.4	0.9	0.6	0.1	1.2	2.7	4.6	7.0	9.5	12.4

Source: cylinder 1 l (matrix: water); distance: 0 cm

$E_\gamma \mid \beta$	5	10	15	20	25	30	35	40	45	50
50	0.9	5.4	10.7	16.6	22.9	29.6	36.8	44.6	52.9	61.8
70	0.5	3.7	7.8	12.3	17.3	22.4	27.9	33.8	39.9	46.4
100	0.2	2.3	5.1	8.6	12.4	16.4	20.7	25.4	30.1	35.2
150	0.1	1.3	3.2	5.7	8.6	11.7	15.2	19.0	22.8	26.9
200	0.1	1.0	2.5	4.6	7.1	9.8	12.8	16.2	19.6	23.4
300	0.0	0.8	2.0	3.8	5.9	8.3	11.0	14.1	17.2	20.7
500	0.0	0.6	1.7	3.3	5.2	7.4	9.8	12.7	15.6	18.9
700	0.0	0.6	1.6	3.1	4.9	6.9	9.3	12.1	14.9	18.1
1000	0.0	0.5	1.5	2.9	4.6	6.5	8.8	11.5	14.3	17.4
1500	0.0	0.5	1.4	2.7	4.3	6.2	8.4	11.0	13.7	16.7
2000	0.0	0.4	1.3	2.6	4.1	6.0	8.2	10.7	13.3	16.4
3000	0.0	0.4	1.2	2.5	4.0	5.8	7.9	10.4	13.0	16.0

Detector: p-type HPGe 500 cm^3

Source: disc 1 cm radius; distance: 10 cm

E_γ | β	5	10	15	20	25	30	35	40	45	50
50	1.9	7.7	14.2	21.5	29.4	38.1	47.7	58.2	69.9	82.6
70	1.2	5.8	11.6	17.9	24.6	32.0	40.0	48.7	58.1	68.3
100	0.6	3.7	8.3	13.5	19.3	25.7	32.5	40.0	47.9	56.6
150	0.3	2.2	5.3	9.3	14.0	19.3	25.1	31.5	38.3	45.8
200	0.2	1.7	4.2	7.5	11.5	16.1	21.3	27.1	33.3	40.2
300	0.2	1.3	3.3	6.1	9.5	13.5	18.1	23.3	28.9	35.1
500	0.1	1.1	2.8	5.1	8.1	11.6	15.8	20.4	25.6	31.3
700	0.1	1.0	2.5	4.7	7.4	10.7	14.6	19.0	23.9	29.4
1000	0.1	0.9	2.3	4.3	6.8	9.9	13.5	17.6	22.3	27.5
1500	0.1	0.8	2.0	3.9	6.2	9.0	12.4	16.3	20.7	25.6
2000	0.1	0.7	1.9	3.6	5.8	8.5	11.8	15.5	19.8	24.6
3000	0.1	0.7	1.8	3.4	5.5	8.1	11.2	14.8	18.9	23.5

Source: Marinelli 5 l (matrix: epoxy)

E_γ | β	5	10	15	20	25	30	35	40	45	50
50	0.1	0.7	1.9	3.4	5.3	7.1	9.2	11.6	14.1	16.8
70	0.1	0.6	1.8	3.4	5.3	7.2	9.3	11.8	14.3	17.1
100	0.2	0.4	1.4	2.9	4.7	6.7	8.8	11.3	13.9	16.7
150	0.2	0.1	0.8	2.1	3.7	5.5	7.5	9.9	12.4	15.2
200	0.2	0.1	0.5	1.6	3.1	4.7	6.7	8.9	11.4	14.0
300	0.3	0.2	0.3	1.2	2.5	4.1	5.9	8.0	10.3	12.9
500	0.3	0.3	0.1	1.0	2.1	3.5	5.2	7.3	9.5	12.0
700	0.3	0.3	0.0	0.8	1.9	3.3	4.9	6.9	9.0	11.5
1000	0.3	0.4	0.1	0.7	1.7	3.0	4.6	6.5	8.6	11.0
1500	0.3	0.4	0.1	0.5	1.5	2.8	4.3	6.2	8.2	10.6
2000	0.3	0.4	0.2	0.5	1.4	2.7	4.2	6.0	8.0	10.3
3000	0.3	0.5	0.2	0.4	1.3	2.5	4.0	5.8	7.8	10.1

Detector: n-type HPGe 100 cm^3

Source: disc 5 cm radius; distance: 0 cm

E_γ | β	5	10	15	20	25	30	35	40	45	50
10	3.6	7.9	12.6	18.2	24.4	31.4	39.2	48.1	58.2	69.5
15	3.5	7.5	12.0	17.3	23.3	30.0	37.5	46.0	55.6	66.4
20	2.6	5.9	9.7	14.4	19.6	25.5	32.1	39.7	48.0	57.5
30	1.6	4.1	7.1	10.9	15.4	20.3	25.9	32.3	39.3	47.1
50	0.7	2.8	5.5	9.0	13.1	17.7	22.8	28.7	35.0	42.2
70	0.1	1.8	4.3	7.6	11.5	16.0	20.9	26.6	32.8	39.7
100	0.5	0.5	2.6	5.4	9.0	13.1	17.7	23.2	29.0	35.6
150	0.9	0.4	1.1	3.3	6.3	9.8	14.0	18.9	24.2	30.4
200	1.1	0.8	0.4	2.4	5.1	8.4	12.3	16.9	22.1	27.9
300	1.2	1.1	0.0	1.7	4.3	7.4	11.1	15.5	20.5	26.1
500	1.2	1.3	0.3	1.3	3.8	6.8	10.3	14.7	19.5	25.0
700	1.3	1.3	0.4	1.1	3.5	6.5	10.0	14.3	19.0	24.5
1000	1.3	1.4	0.6	1.0	3.3	6.2	9.7	13.9	18.6	24.1
1500	1.4	1.5	0.7	0.8	3.1	6.0	9.4	13.6	18.3	23.7
2000	1.4	1.5	0.7	0.7	3.0	5.8	9.2	13.4	18.1	23.5
3000	1.4	1.6	0.8	0.7	2.9	5.7	9.1	13.3	17.9	23.3

Source: cylinder 100 ml (matrix: water); distance: 0 cm

E_γ | β	5	10	15	20	25	30	35	40	45	50
10	2.8	6.3	10.2	14.9	20.1	26.0	32.6	40.0	48.2	57.5
15	3.3	7.1	11.3	16.2	21.6	27.5	34.1	41.4	49.5	58.5
20	3.6	7.6	12.0	17.0	22.5	28.6	35.3	42.7	50.8	59.8
30	3.6	7.8	12.5	17.7	23.4	29.6	36.5	44.0	52.2	61.3
50	2.8	7.0	11.6	16.8	22.6	28.8	35.7	43.2	51.4	60.5
70	1.8	5.4	9.7	14.7	20.3	26.4	33.0	40.4	48.4	57.3
100	1.0	3.5	6.9	11.1	16.0	21.5	27.6	34.4	41.9	50.2
150	0.6	2.2	4.6	7.8	11.7	16.2	21.3	27.1	33.6	40.8
200	0.4	1.8	3.8	6.6	10.0	14.0	18.5	23.8	29.7	36.3
300	0.3	1.5	3.3	5.7	8.7	12.3	16.5	21.3	26.8	32.9
500	0.3	1.3	2.9	5.2	8.0	11.3	15.2	19.7	24.8	30.7
700	0.3	1.2	2.8	4.9	7.6	10.8	14.6	19.0	23.9	29.6
1000	0.2	1.2	2.6	4.7	7.3	10.4	14.0	18.3	23.1	28.6
1500	0.2	1.1	2.5	4.5	7.0	10.0	13.5	17.6	22.3	27.7
2000	0.2	1.0	2.4	4.3	6.8	9.7	13.2	17.3	21.9	27.2
3000	0.2	1.0	2.4	4.2	6.6	9.5	12.9	16.9	21.5	26.7

Detector: n-type HPGe 200 cm^3

Source: point; distance: 0 cm

E_γ | β	5	10	15	20	25	30	35	40	45	50
10	0.8	1.9	2.7	4.0	5.5	7.1	9.1	11.4	14.3	17.5
15	0.9	2.0	2.7	4.1	5.6	7.2	9.1	11.4	14.3	17.7
20	0.9	2.1	3.0	4.4	6.0	7.8	9.8	12.3	15.4	18.8
30	0.9	2.2	3.1	4.6	6.2	8.1	10.2	12.8	16.0	19.4
50	0.7	2.0	2.9	4.4	6.0	7.9	10.0	12.6	15.9	19.3
70	0.6	1.6	2.6	4.0	5.6	7.4	9.5	12.0	15.2	18.8
100	0.4	1.2	2.1	3.4	4.9	6.5	8.5	10.8	13.7	17.2
150	0.2	0.8	1.5	2.6	3.8	5.3	7.0	9.1	11.6	14.7
200	0.2	0.6	1.3	2.2	3.3	4.7	6.2	8.1	10.4	13.2
300	0.1	0.5	1.1	1.9	2.9	4.1	5.6	7.3	9.4	12.0
500	0.1	0.5	1.0	1.7	2.6	3.8	5.1	6.7	8.7	11.0
700	0.1	0.4	0.9	1.6	2.5	3.6	4.9	6.4	8.3	10.5
1000	0.1	0.4	0.8	1.5	2.4	3.4	4.6	6.1	7.9	10.1
1500	0.1	0.4	0.8	1.4	2.2	3.2	4.4	5.8	7.6	9.6
2000	0.1	0.4	0.8	1.4	2.2	3.1	4.3	5.7	7.4	9.4
3000	0.1	0.3	0.7	1.3	2.1	3.0	4.2	5.5	7.2	9.1

Source: Marinelli 1 l (matrix: epoxy)

E_γ | β	5	10	15	20	25	30	35	40	45	50
10	1.3	5.1	9.1	13.9	18.9	24.3	87.0	37.0	38.0	52.9
15	0.9	3.9	6.3	9.7	12.7	16.7	100	24.2	100	33.4
20	0.0	1.6	3.1	5.0	7.0	9.1	60.7	13.8	100	19.2
30	0.3	0.4	1.2	2.4	3.9	5.3	6.8	8.7	9.9	12.6
50	0.2	0.3	1.0	2.2	3.6	5.1	6.7	8.5	10.4	12.5
70	0.2	0.3	1.1	2.3	3.9	5.4	7.2	9.2	11.3	13.5
100	0.2	0.1	0.8	1.9	3.4	5.0	6.8	8.9	11.1	13.4
150	0.2	0.2	0.3	1.2	2.5	3.9	5.6	7.5	9.6	11.9
200	0.2	0.2	0.1	0.9	2.0	3.3	4.9	6.7	8.7	11.0
300	0.2	0.3	0.0	0.6	1.6	2.8	4.3	6.1	8.0	10.1
500	0.2	0.4	0.1	0.4	1.3	2.5	3.9	5.6	7.5	9.6
700	0.2	0.4	0.2	0.4	1.2	2.3	3.7	5.4	7.2	9.3
1000	0.2	0.4	0.2	0.3	1.1	2.2	3.6	5.2	7.0	9.1
1500	0.2	0.4	0.3	0.2	1.0	2.1	3.4	5.0	6.8	8.9
2000	0.2	0.5	0.3	0.2	0.9	2.0	3.3	4.9	6.7	8.8
3000	0.2	0.5	0.3	0.1	0.9	1.9	3.2	4.8	6.6	8.7

Detector: n-type HPGe 500 cm^3

Soruce: disc 5 cm radius; distance: 20 cm

E_γ | β	5	10	15	20	25	30	35	40	45	50
10	3.7	7.7	11.8	16.1	20.6	25.4	30.3	35.5	40.9	46.6
15	3.8	7.8	12.0	16.4	21.0	25.9	31.0	36.3	41.8	47.7
20	3.8	7.7	11.8	16.2	20.7	25.5	30.4	35.7	41.1	46.8
30	3.6	7.6	11.6	15.9	20.4	25.1	30.0	35.2	40.6	46.2
50	3.2	7.1	11.1	15.4	19.8	24.5	29.4	34.5	39.8	45.4
70	2.7	6.4	10.3	14.5	18.9	23.6	28.4	33.4	38.7	44.3
100	1.9	5.1	8.8	12.8	17.0	21.5	26.2	31.2	36.3	41.8
150	1.2	3.7	6.8	10.4	14.2	18.4	22.8	27.4	32.3	37.5
200	1.0	3.1	5.8	9.0	12.6	16.5	20.6	25.0	29.7	34.7
300	0.8	2.6	4.9	7.8	11.1	14.7	18.6	22.7	27.2	31.9
500	0.7	2.2	4.3	7.0	10.0	13.3	17.0	20.9	25.2	29.7
700	0.6	2.0	4.0	6.5	9.4	12.6	16.1	20.0	24.1	28.5
1000	0.6	1.9	3.8	6.1	8.8	11.9	15.3	19.1	23.1	27.4
1500	0.5	1.7	3.5	5.7	8.3	11.3	14.5	18.1	22.1	26.3
2000	0.5	1.7	3.3	5.5	8.0	10.9	14.1	17.6	21.5	25.6
3000	0.5	1.6	3.2	5.2	7.7	10.5	13.6	17.1	20.9	25.0

Source: cylinder 1 l (matrix: epoxy); distance: 0 cm

E_γ | β	5	10	15	20	25	30	35	40	45	50
10	2.8	6.4	11.0	16.3	22.7	29.9	38.3	47.8	58.6	71.0
15	2.8	6.4	10.8	15.9	21.8	28.6	36.3	45.2	55.1	66.5
20	2.5	5.8	9.7	14.4	19.9	26.1	33.1	41.1	50.0	60.2
30	2.2	5.1	8.7	12.9	17.8	23.3	29.4	36.4	44.1	52.7
50	1.9	4.9	8.4	12.5	17.2	22.5	28.3	34.8	41.9	49.8
70	1.3	4.1	7.6	11.7	16.3	21.5	27.2	33.6	40.6	48.3
100	0.6	2.8	5.9	9.7	14.1	19.1	24.6	30.7	37.6	45.0
150	0.1	1.6	3.9	7.1	10.9	15.4	20.4	26.1	32.4	39.4
200	0.1	1.0	3.1	5.8	9.3	13.4	18.0	23.3	29.2	35.8
300	0.2	0.7	2.4	4.8	7.9	11.7	15.9	20.8	26.4	32.6
500	0.3	0.4	2.0	4.1	7.0	10.5	14.4	19.0	24.3	30.1
700	0.3	0.3	1.8	3.8	6.5	9.9	13.7	18.1	23.2	28.8
1000	0.4	0.2	1.6	3.5	6.1	9.3	13.0	17.3	22.2	27.7
1500	0.4	0.1	1.4	3.2	5.7	8.7	12.3	16.4	21.1	26.5
2000	0.4	0.1	1.3	3.1	5.5	8.4	11.9	15.9	20.6	25.8
3000	0.4	0.0	1.2	2.9	5.2	8.1	11.5	15.5	20.0	25.2

- 100 cm^3 p-type HPGe detector: H = 52 mm, R_0 = 26 mm, ρ = 7.8 mm, *i. e.* ρ/R_0 = 30%; 100 cm^3 cylindrical source (matrix: water), positioned at the detector top, *i. e.* distance = 0; errors (when not taking bulletization into account) are as high as 26% for 50 keV, 18% for 100 keV, and 8% for 1000 keV,
- 100 cm^3 n-type HPGe detector: H = 52 mm, R_0 = 25 mm, ρ = 1.2 mm (slight/minimal bulletization), *i. e.* ρ/R_0 = 5%; 5 cm radius disc source at the detector top; errors are negligible at higher energies, but still 2-4% at low energies,
- 200 cm^3 n-type HPGe detector: H = 63 mm, R_0 = 32 mm, ρ = 8 mm, *i. e.* ρ/R_0 = 25%; 1000 cm^3 Marinelli source (matrix: epoxy resin); errors are 19% for 10 keV, 7% for 20 keV, 3% for 100 keV and 1% for 1000 keV, and
- thick LEPD: H = 20 mm, R_0 = 18 mm, ρ = 9 mm, *i. e.* ρ/R_0 = 50% ; point source at 10 cm distance from the detector end-cap; errors are 31-46% in the energy range of interest.

Although it was not the aim of this work to analyse in detail the results obtained, some general conclusions on the bulletization effect could be made:

- there is an approximately quadratic δ *vs*. ρ/R_0 dependence (fig. 10); this is due to quadratic dependence on ρ of the removed (when rounded) part of the crystal *vs*. whole crystal volume,
- the effect is not negligible even for only slightly/minimally bulletized detectors (*e. g.* ρ/R_0 = 5%),
- for extreme bulletization (ρ/R_0 > 50%) the above quadratic dependence leads to extreme errors; this is, however, more of theoretical than practical nature,
- effect is more prominent at lower energies (figs. 9 and 10); it is therefore particularly important for LEPD and n-type HPGe detectors,

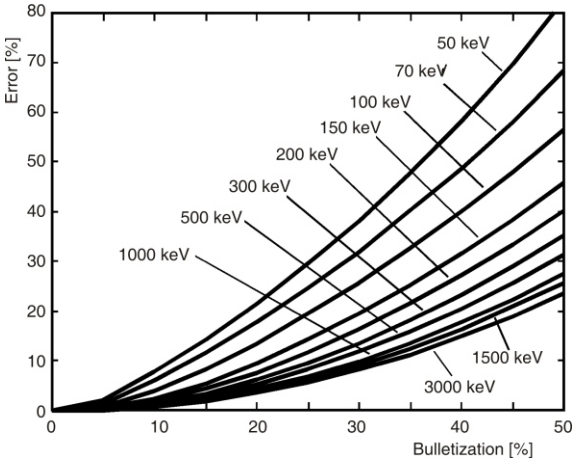

Figure 10. Illustration of δ *vs.* ρ/R_0 quadratic dependence for several gamma-energies (detector: p-type HPGe 500 cm^3; source: disc, 1 cm radius; source-to-detector distance: 10 cm)

- it is slightly more prominent for smaller sources;
- it is not much dependent on source matrix,
- the effect tends to be more prominent for close geometries; however, for some counting arrangements, it is most prominent not at the closest one (source placed on the top of the detector), but at a somewhat higher one; then decreases at positions further away, and
- as previously noted, bulletization impact will tend to reduce when applying ET principle, *i. e.* when comparing efficiency of the sample to that of the reference source; if so, the impact can be estimated by comparing (subtracting) the δ-values for the two; when sample is similar to the reference/standard source and both are counted in the same conditions, their δ-difference will tend to zero, regardless of bulletization ("near-relative" method of quantitative gamma-spectrometry, featuring in ANGLE).

Results obtained and the above conclusions are not surprising – these are readily explicable by the physical nature of gamma-spectrometry process. The same conclusions are, of course, valid regardless of the modality of calculations applied. In the present work it went about the exact mathematical/analytical treatment – effective solid angle ($\overline{\Omega}$) – incorporating geometrical solid angle, gamma emission in the source, attenuation in the intercepting materials, including source matrix and detector response, eqs. (1) and (2); similar findings when applying statistical MC approaches (although fragmentary and on simplified bulletization models) are reported elsewhere [7-10].

Readers interested in more elaborate conclusions may wish to explore the results which are available for download in full detail in ref. [44], or to produce new/targeted ones using the above approach/modelling and/or ANGLE software.

CONCLUSIONS

When applying absolute or semi-empirical methods for full energy peak efficiency calculations, detector should be described in as much detail as possible. Among many parameters characterizing the detector, crystal edge rounding (bulletization) is most often neglected, leading to systematic errors which may be considerable – even unacceptable (tens of percent) – especially for low gamma energies and close counting geometries. The error made by not taking bulletization into account is sharply increasing with the extent of bulletization (bulletization radius) and with decreasing energy.

In the present work the problem is mathematically/analytically solved – relevant formulae are derived and subsequently programmed for numerical calculations. This is now part of the commercially available ANGLE 3 software. Extensive calculation

testing (for more than 150 000 situations), with varying source, detector and counting geometry data, performed in 10-3000 keV energy range, yielded valuable evidence about the impact of detector bulletization on gamma-efficiency. Analysts can compare their respective counting arrangements with these data so as to get an idea of if/how to tackle the problem.

From the other side, ET approach in efficiency calculations – intrinsic of ANGLE – is a good remedy against incorrect (or poorly known) detector data, bulletization included. ET tends to reduce error propagation from these data into calculated efficiency. This is particularly the case when actual source (shape, size, matrix) and counting arrangement (distance, intercepting layers) are closely similar to the reference/standard ones, *i. e*. in "near-relative" method of quantitative gamma-spectrometry, as applied in ANGLE software.

REFERENCES

[1] ORTEC Online Catalogue, www.ortec-online.com/solutions/index.aspx
[2] Canberra Online Catalogue, www.canberra.com/products
[3] Debertin, K. R, Helmer, G., Gamma- and X-ray Spectrometry with Semiconductor Detectors, North-Holland, New York, USA, 1988
[4] Knoll, G. F, Radiation Detection and Measurement, 3rd ed., John Wiley & Sons, New York, USA, 2000
[5] Gilmore, G. R, Practical Gamma-Ray Spectrometry, 2nd ed. John Wiley & Sons, New York, USA, 2008
[6] Mayer, S., *et al*., Characterisation of the PSI Whole Body Counter by Radiographic Imaging, *Radiation Protection Dosimetry, 144* (2011), 1-4, pp. 398-401
[7] Boson, J., Agren, G., Johansson, L., A Detailed Investigation of HPGe Detector Response for Improved Monte Carlo Efficiency Calculations, *Nucl. Instrum. Methods Phys. Res. A, 587* (2008), 2-3, pp. 304-314
[8] Gasparro, J., *et al*., Monte Carlo Modelling of Germanium Crystals that Are Tilted and Have Rounded Front Edges, *Nucl. Instrum. Methods. Phys. Res. A, 594* (2008), 2, pp. 196-201
[9] Ashrafi, S., Likar, A., Vidmar, T., Precise Modeling of a Coaxial HPGe Detector, *Nucl. Instrum. Methods Phys. Res. A, 438* (1999), 2-3, pp. 421-428, 1999
[10] Vidmar, T., Gasparro, J., Crystal Rounding and the Efficiency Transfer Method in Gamma-Ray Spectrometry, *Appl. Radiat. Isot., 67* (2009), 11, pp. 2057-2061
[11] Lepy, M. C., *et al*., Intercomparison of Efficiency Transfer Software for Gamma-Ray Spectrometry, *Appl. Radiat. Isot., 55* (2001), 4, pp. 493-503
[12] Hardy, J. C., *et al*., Precise Efficiency Calibration of an HPGe Detector: Source Measurements and Monte Carlo Calculations with Sub-Percent Precision, *Appl. Radiat. Isot., 56* (2002), 1-2, pp. 65-69
[13] Moens, L., Debertin, K., The Need for Cylindrical Germanium Gamma-Ray Detectors with Accurately Specified Dimensions, *Nucl. Instrum. Methods Phys. Res. A, 238* (1985), 1, pp. 180-181
[14] Fechner, M., *et al.*, A Large HPGe Detector for the Non-Destructive Radioassay of an Ultra-Low-Background Counting Facility, *Appl. Radiat. Isot., 69* (2011), 7, pp. 1033-1038
[15] Moens, L., *et al.*, Calculation of the Absolute Peak Efficiency of Gamma-Ray Detectors for Different Counting Geometries, *Nucl. Instrum. Methods Phys. Res., 187* (1981), 2-3, pp. 451-472
[16] Jovanović, S., *et al.*, ANGLE: A PC-Code for Semiconductor Detector Efficiency Calculations, *J. Radioanal. Nucl. Chem., 218* (1997), 1, pp. 13-20
[17] Vukotić, P., *et al*., On the Applicability of the Effective Solid Angle Concept in Activity Determination of Large Cylindrical Sources, *J. Radioanal. Nucl. Chem., 218* (1997), 1, pp. 21-26
[18] Sima, O., Arnold, D., Transfer of the Efficiency Calibration of Germanium Gamma-Ray Detectors Using the GESPECOR Software, *Appl. Rad. Isot., 56* (2002), 1-2, pp. 71-75
[19] Piton, F., Lepy, M. C., Be, M. M., Plagnard, J., Efficiency Transfer and Coincidence Summing Corrections for γ-Ray Spectrometry, *Appl. Radiat. Isot., 52* (2000), 3, pp.791-795
[20] Cornejo Dyaz, N., Jurado Vargas, M., DETEFF: An Improved Monte Carlo Computer Program for Evaluating the Efficiency in Coaxial Gamma-Ray Detectors, *Nucl. Instrum. Methods Phys. Res. A., 586* (2008), 2, pp. 204-210
[21] Vidmar, T., EFFTRAN – A Monte Carlo Efficiency Transfer Code for Gamma-Ray Spectrometry, *Nucl. Instrum. Methods Phys. Res. A, 550* (2005), 3, pp. 603-608
[22] Vidmar, T., *et al*., An Intercomparison of Monte Carlo Codes Used in Gamma-Ray Spectrometry, *Appl. Radiat. Isot., 66* (2008), 6-7, pp. 764-768
[23] Hurtado, S., Villa, M., An Intercomparison of Monte Carlo Codes Used for *In-Situ* Gamma-Ray Spectrometry, *Rad. Meas., 45* (2010), 8, pp. 923-927
[24] Jackman, K. R., Biegalski, R., Methods and Software for Predicting Germanium Detector Absolute Full-Energy Peak Efficiencies, *J. Radioanal. Nucl. Chem., 279* (2009), 1, pp. 355-360
[25] Jackman, K. R., KMESS: An Open Source Software Package Using a Semi-Empirical Mesh-Grid Method for the Modeling of Germanium Detector Efficiencies, Ph. D. thesis, University of Texas, Austin, USA., 2007
[26] Abbas, K., *et al*., Reliability of Two Calculation Codes for Efficiency Calibrations of HPGe Detectors, *Appl. Radiat. Isot., 56* (2002), 5, pp. 703-709
[27] Vidmar, T., *et al*., Testing Efficiency Transfer Codes for Equivalence, *Appl. Radiat. Isot., 68* (2010), 2, pp. 355-359
[28] Jovanović, S., Dlabač, A., Mihaljević, N., ANGLE v2.1 – New Version of the Computer Code for Semiconductor Detector Gamma-Efficiency Calculations, *Nucl. Instrum. Methods Phys. Res. A, 622* (2010), 2, pp. 385-391
[29] Steljić, M., Milosević, M., Beličev, P., Modeling of Germanium Detector and Its Sourceless Calibration, *Nucl Technol Radiat, 23* (2008), 2, pp. 51-57
[30] Vukašinović, I., Todorović, D., Popović, D., The Dependence of Ge Detectors Efficiency on the Density of the Samples in Gamma-ray Spectrometry, *Nucl Technol Radiat, 22* (2007), 2, pp. 58-63
[31] Novković, D., *et al*., The Direct Activity Measurement of ^{133}Ba by Using HPGe Spectrometer, *Nucl Technol Radiat, 26* (2011), 1, pp. 64-68
[32] Jovanović, S., Dlabač, A., ANGLE Software, angle.dlabac.com
[33] ***, ORTEC Applications Software, ANGLE Software, http://www.ortec-online.com/Solutions/Software/index.aspx?tab=3#Angle
[34] Jovanović, S., Dlabač, A., Mihaljević, N., ANGLE v2.1 – New Version of the Computer Code for Semi-

conductor Detector Gamma-Efficiency Calculations, Paper Presented at the 5th International k_0-Users Workshop, Belo Horizonte, Brazil, September 13-17, 2009
[35] Andreev, D. S., *et al*., Consideration of Cascade Transitions in Determining the Absolute Yield of Gamma-Rays, *Instr. Expt. Techn., 15* (1972), 9, pp. 1358-1359
[36] Moens, L., *et al*., Calculation of the Absolute Peak Efficiency of Ge and Ge(Li) Detectors for Different Counting Geometries, *J. Radioanal. Chem., 70* (1982), 1-2, pp. 539-550
[37] Moens, L., Hoste, J., Calculation of the Peak Efficiency of High-Purity Germanium Detectors, *Appl. Radiat. Isot., 34* (1983), 8, pp. 1085-1095
[38] Mihaljević, N., *et al*., Calculation of Full Energy Peak Detection Efficiencies of Semiconductor Detectors for Some Interesting Counting Geometries, *Proceedings,* International k_0-Users Workshop, 1992, Gent, Astene, Belgium, pp. 53-57
[39] Jovanović, S., *et al*., Experimental Test of MARSANGLE, A Computer Code to Calculate Detection Efficiencies of Ge-Detectors for Marinelli Sources, *Proceedings*, International k_0-Users Workshop, 1992, Gent, Astene, Belgium, pp. 59-62
[40] Mihaljević, N., *et al*., "EXTSANGLE" – An Extension of the Efficiency Conversion Program "SOLANG" to Sources with a Diameter Larger than that of the Ge-detector, *J. Radioanal. Nucl. Chem., 169* (1993), 1, pp. 209-218
[41] Erten, H. N., Aksoyoglu, S., Gokturk, H., Efficiency Calibration and Summation Effects in Gamma-Ray Spectrometry, *J. Radioanal. Nucl. Chem., 125* (1988), 1, pp. 3-10
[42] Vidmar, T., Likar, A., On the Invariability of the Total-to-Peak Ratio in Gamma-Ray Spectrometry, *Appl. Radiat. Isot., 60* (2004), 2-4, pp. 191-195
[43] Faddeev, D. K., Lessons on Algebra (in Russian), Nauka, Moscow, 1970
[44] Dlabač, A., Jovanović, S., Numerical Results of the Study on the Effect of Bulletization on HPGe Detector Gamma-Efficiency Calculations, http://angle.dlabac.com/bulletization_study.html

Received on September 19, 2011
Accepted on January 24, 2012

Никола МИХАЉЕВИЋ, Александар ДЛАБАЧ, Слободан ЈОВАНОВИЋ

УТИЦАЈ ЗАОБЉЕЊА КРИСТАЛА ДЕТЕКТОРА НА ИЗРАЧУНАВАЊЕ ЕФИКАСНОСТИ ДЕТЕКЦИЈЕ ГАМА-ЗРАЧЕЊА – ТЕОРИЈСКА РАЗРАДА И ПРИМЕНА У СОФТВЕРУ ANGLE

Приликом израчунавања ефикасности полупроводничких детектора гама-зрачења помоћу апсолутних или (полу)емпиријских метода, потребно је веома детаљно знати конструкционе карактеристике детектора – димензије и распоред/конфигурације појединих делова, материјале од којих су направљени, итд. Заобљење кристала детектора, уколико се занемари (што је најчешће случај), може проузроковати значајну систематску грешку у прорачуну ефикасности. Ово нарочито долази до изражаја на ниским гама-енергијама и тзв. блиским геометријама (мала растојања извора зрачења од детектора). Грешке расту са квадратом полупречника заобљења кристала. Математичко/аналитичко решење проблема до сада није било познато и елаборирано је у овом раду по први пут. Изведени су математички изрази којима се заобљење узима у обзир приликом прорачуна ефикасности детектора, и то за неколико карактеристичних (у пракси најчешћих) случајева гама-спектрометријских мерења: извори у облику тачке, диска, цилиндра и Маринели тип. Изведени изрази су веома комплексни и програмирани су потом за нумеричко рачунање у оквиру комерцијалног софтвера ANGLE. Детаљна провера прорачуна урађена је за чисто германијумске (HPGe) детекторе n- и p-типа, као и за нискоенергетске детекторе (LEPD). За сваки тип детектора узето је у обзир неколико величина, као и много различитих извора, на различитим растојањима од детектора (0-20 cm). Посматран је енергетски опсег гама зрачења 10-3000 keV. Да би се истакао значај питања заобљења детектора, урађена је обимна студија пропагације грешке: резултати прорачуна ефикасности са узимањем заобљења у обзир и без тога систематски су сређени и упоређени. Одговарајуће грешке су табеларно дате у исцрпној Excel датотеци (више од 152 000 резултата). Датотека се може преузети са посебног сајта, а мањи број карактеристичних резултата је изабран и приказан у раду. ANGLE се показао веома практичним приликом програмирања овог задатка и брзим током прорачуна. Добијени резултати убедљиво илуструју утицај заобљења кристала детектора, а тиме и потребу да се узму у обзир приликом рачунања ефикасности. Чак и мало заобљење (полупречника 1-2 mm) није занемарљиво у многим реалним мерењима. Читалац, гама-спектрометрист може сада (1) да упореди своју мерну конфигурацију са подацима из овог рада и тиме стекне представу о величини проблема (тј. своје систематске грешке), и (2) да примени описани математички модел и/или ANGLE софтвер да реши проблем.

Кључне речи: заобљење кристала детектора, полупроводнички детектори, прорачун ефикасности, пропагација грешке, ANGLE софтвер, гама спектрометрија